Article:

Search for Astrophysical Electron Antineutrinos in Super-Kamiokande with 0.01% Gadolinium-loaded Water

M. Harada[1], K. Abe[2,3], C. Bronner[2], Y. Hayato[2,3], K. Hiraide[2,3], K. Hosokawa[2], K. Ieki[2,3], M. Ikeda[2,3],
J. Kameda[2,3], Y. Kanemura[2], R. Kaneshima[2], Y. Kashiwagi[2], Y. Kataoka[2,3], S. Miki[2], S. Mine[2,4], M. Miura[2,3], S. Moriyama[2,3],
Y. Nakano[2], M. Nakahata[2,3], S. Nakayama[2,3], Y. Noguchi[2], K. Okamoto[2], K. Sato[2], H. Sekiya[2,3], H. Shiba[2],
K. Shimizu[2], M. Shiozawa[2,3], Y. Sonoda[2], Y. Suzuki[2], A. Takeda[2,3], Y. Takemoto[2,3], A. Takenaka[2], H. Tanaka[2,3],
S. Watanabe[2], T. Yano[2], S. Han[5], T. Kajita[3,5,6], K. Okumura[3,5], T. Tashiro[5], T. Tomiya[5], X. Wang[5], S. Yoshida[5],
G. D. Megias[7], P. Fernandez[8], L. Labarga[8], N. Ospina[8], B. Zaldivar[8], B. W. Pointon[9,10], E. Kearns[3,11], J. L. Raaf[11],
L. Wan[11], T. Wester[11], J. Bian[4], N. J. Griskevich[4], S. Locke[4], M. B. Smy[3,4], H. W. Sobel[3,4], V. Takhistov[4,12],
A. Yankelevich[4], J. Hill[13], S. H. Lee[14], D. H. Moon[14], R. G. Park[14], B. Bodur[15], K. Scholberg[3,15], C. W. Walter[3,15],
A. Beauchêne[16], O. Drapier[16], A. Giampaolo[16], Th. A. Mueller[16], A. D. Santos[16], P. Paganini[16], B. Quilain[16], T. Ishizuka[17],
T. Nakamura[18], J. S. Jang[19], J. G. Learned[20], K. Choi[21], N. Iovine[21], S. Cao[22], L. H. V. Anthony[23], D. Martin[23], M. Scott[23],
A. A. Sztuc[23], Y. Uchida[23], V. Berardi[24], M. G. Catanesi[24], E. Radicioni[24], N. F. Calabria[25], A. Langella[25],
L. N. Machado[25], G. De Rosa[25], G. Collazuol[26], F. Iacob[26], M. Lamoureux[26], M. Mattiazzi[26], L. Ludovici[27], M. Gonin[6],
G. Pronost[6], C. Fujisawa[28], Y. Maekawa[28], Y. Nishimura[28], R. Okazaki[28], R. Akutsu[12], M. Friend[12], T. Hasegawa[12],
T. Ishida[12], T. Kobayashi[12], M. Jakkapu[12], T. Matsubara[12], T. Nakadaira[12], K. Nakamura[3,12], Y. Oyama[12], K. Sakashita[12],
T. Sekiguchi[12], T. Tsukamoto[12], N. Bhuiyan[29], G. T. Burton[29], F. Di Lodovico[29], J. Gao[29], A. Goldsack[29], T. Katori[29],
J. Migenda[29], Z. Xie[29], S. Zsoldos[3,29], Y. Kotsar[30], H. Ozaki[30], A. T. Suzuki[30], Y. Takagi[30], Y. Takeuchi[3,30], J. Feng[31],
L. Feng[31], J. R. Hu[31], Z. Hu[31], T. Kikawa[31], M. Mori[31], T. Nakaya[3,31], R. A. Wendell[3,31], K. Yasutome[31],
S. J. Jenkins[32], N. McCauley[32], P. Mehta[32], A. Tarrant[32], Y. Fukuda[33], Y. Itow[34,35], H. Menjo[34], K. Ninomiya[34],
J. Lagoda[36], S. M. Lakshmi[36], M. Mandal[36], P. Mijakowski[36], Y. S. Prabhu[36], J. Zalipska[36], M. Jia[37], J. Jiang[37], C. K. Jung[37],
M. J. Wilking[37], C. Yanagisawa[37,56], Y. Hino[1], H. Ishino[1], H. Kitagawa[1], Y. Koshio[1,3], F. Nakanishi[1], S. Sakai[1],
T. Tada[1], T. Tano[1], G. Barr[38], D. Barrow[38], L. Cook[3,38], S. Samani[38], D. Wark[38,39], A. Holin[40], F. Nova[41], B. S. Yang[40],
J. Y. Yang[40], J. Yoo[40], J. E. P. Fannon[42], L. Kneale[42], M. Malek[42], J. M. McElwee[42], M. D. Thiesse[42], L. F. Thompson[42],
S. T. Wilson[42], H. Okazawa[43], S. B. Kim[44], E. Kwon[44], J. W. Seo[44], I. Yu[44], A. K. Ichikawa[45], K. D. Nakamura[45],
S. Tairafune[45], K. Nishijima[46], K. Nakagiri[47], Y. Nakajima[3,47], S. Shima[47], N. Taniuchi[47], E. Watanabe[47],
M. Yokoyama[3,47], P. de Perio[3], K. Martens[3], K. M. Tsui[3], M. R. Vagins[3,4], J. Xia[3], M. Kuze[48], S. Izumiyama[48],
R. Matsumoto[48], M. Ishitsuka[49], H. Ito[49], T. Kinoshita[49], R. Matsumoto[49], Y. Ommura[49], N. Shigeta[49], M. Shinoki[49],
T. Suganuma[49], K. Yamauchi[49], J. F. Martin[50], H. A. Tanaka[50], T. Towstego[50], R. Gaur[10], V. Gousy-Leblanc[10,57], M. Hartz[10],
A. Konaka[10], X. Li[10], N. W. Prouse[10,51], S. Chen[51], B. D. Xu[51], B. Zhang[51], M. Posiadala-Zezula[52], S. B. Boyd[53],
R. Edwards[53], D. Hadley[53], M. Nicholson[53], M. O'Flaherty[53], B. Richards[53], A. Ali[10,54], B. Jamieson[54], Ll. Marti[55],
A. Minamino[55], G. Pintaudi[55], S. Sano[55], S. Suzuki[55], K. Wada[55], and
The Super-Kamiokande Collaboration

[1] Department of Physics, Okayama University, Okayama, Okayama 700-8530, Japan; pc3g4sej@s.okayama-u.ac.jp
[2] Kamioka Observatory, Institute for Cosmic Ray Research, University of Tokyo, Kamioka, Gifu 506-1205, Japan
[3] Kavli Institute for the Physics and Mathematics of the Universe (WPI), The University of Tokyo Institutes for Advanced Study, University of Tokyo, Kashiwa, Chiba 277-8583, Japan
[4] Department of Physics and Astronomy, University of California, Irvine, CA 92697-4575, USA
[5] Research Center for Cosmic Neutrinos, Institute for Cosmic Ray Research, University of Tokyo, Kashiwa, Chiba 277-8582, Japan
[6] ILANCE, CNRS - University of Tokyo International Research Laboratory, Kashiwa, Chiba 277-8582, Japan
[7] Institute for Cosmic Ray Research, University of Tokyo, Kashiwa, Chiba 277-8582, Japan
[8] Department of Theoretical Physics, University Autonoma Madrid, E-28049 Madrid, Spain
[9] Department of Physics, British Columbia Institute of Technology, Burnaby, BC, V5G 3H2, Canada
[10] TRIUMF, 4004 Wesbrook Mall, Vancouver, BC, V6T2A3, Canada
[11] Department of Physics, Boston University, Boston, MA 02215, USA
[12] High Energy Accelerator Research Organization (KEK), Tsukuba, Ibaraki 305-0801, Japan
[13] Department of Physics, California State University, Dominguez Hills, Carson, CA 90747, USA
[14] Institute for Universe and Elementary Particles, Chonnam National University, Gwangju 61186, Republic of Korea
[15] Department of Physics, Duke University, Durham, NC 27708, USA
[16] Ecole Polytechnique, IN2P3-CNRS, Laboratoire Leprince-Ringuet, F-91120 Palaiseau, France
[17] Junior College, Fukuoka Institute of Technology, Fukuoka, Fukuoka 811-0295, Japan
[18] Department of Physics, Gifu University, Gifu, Gifu 501-1193, Japan
[19] GIST College, Gwangju Institute of Science and Technology, Gwangju 500-712, Republic of Korea
[20] Department of Physics and Astronomy, University of Hawaii, Honolulu, HI 96822, USA
[21] Institute for Basic Science (IBS), Daejeon 34126, Republic of Korea
[22] Institute For Interdisciplinary Research in Science and Education, ICISE, Quy Nhon 55121, Vietnam
[23] Department of Physics, Imperial College London, London SW7 2AZ, UK
[24] Dipartimento Interuniversitario di Fisica, INFN Sezione di Bari and Università e Politecnico di Bari, I-70125, Bari, Italy
[25] Dipartimento di Fisica, INFN Sezione di Napoli and Università di Napoli, I-80126, Napoli, Italy
[26] Dipartimento di Fisica, INFN Sezione di Padova and Università di Padova, I-35131, Padova, Italy
[27] INFN Sezione di Roma and Università di Roma "La Sapienza," I-00185, Roma, Italy

[28] Department of Physics, Keio University, Yokohama, Kanagawa, 223-8522, Japan
[29] Department of Physics, King's College London, London WC2R 2LS, UK
[30] Department of Physics, Kobe University, Kobe, Hyogo 657-8501, Japan
[31] Department of Physics, Kyoto University, Kyoto, Kyoto 606-8502, Japan
[32] Department of Physics, University of Liverpool, Liverpool L69 7ZE, UK
[33] Department of Physics, Miyagi University of Education, Sendai, Miyagi 980-0845, Japan
[34] Institute for Space-Earth Environmental Research, Nagoya University, Nagoya, Aichi 464-8602, Japan
[35] Kobayashi-Maskawa Institute for the Origin of Particles and the Universe, Nagoya University, Nagoya, Aichi 464-8602, Japan
[36] National Centre For Nuclear Research, 02-093 Warsaw, Poland
[37] Department of Physics and Astronomy, State University of New York at Stony Brook, NY 11794-3800, USA
[38] Department of Physics, Oxford University, Oxford OX1 3PU, UK
[39] STFC, Rutherford Appleton Laboratory, Harwell Oxford, and Daresbury Laboratory, Warrington OX11 0QX, UK
[40] Department of Physics, Seoul National University, Seoul 151-742, Republic of Korea
[41] Rutherford Appleton Laboratory, Harwell, Oxford OX11 0QX, UK
[42] Department of Physics and Astronomy, University of Sheffield, Sheffield S3 7RH, UK
[43] Department of Informatics in Social Welfare, Shizuoka University of Welfare, Yaizu, Shizuoka, 425-8611, Japan
[44] Department of Physics, Sungkyunkwan University, Suwon 440-746, Republic of Korea
[45] Department of Physics, Faculty of Science, Tohoku University, Sendai, Miyagi 980-8578, Japan
[46] Department of Physics, Tokai University, Hiratsuka, Kanagawa 259-1292, Japan
[47] Department of Physics, University of Tokyo, Bunkyo, Tokyo 113-0033, Japan
[48] Department of Physics, Tokyo Institute of Technology, Meguro, Tokyo 152-8551, Japan
[49] Department of Physics, Faculty of Science and Technology, Tokyo University of Science, Noda, Chiba 278-8510, Japan
[50] Department of Physics, University of Toronto, ON, M5S 1A7, Canada
[51] Department of Engineering Physics, Tsinghua University, Beijing 100084, People's Republic of China
[52] Faculty of Physics, University of Warsaw, Warsaw 02-093, Poland
[53] Department of Physics, University of Warwick, Coventry CV4 7AL, UK
[54] Department of Physics, University of Winnipeg, MB R3J 3L8, Canada
[55] Department of Physics, Yokohama National University, Yokohama, Kanagawa 240-8501, Japan

Abstract

We report the first search result for the flux of astrophysical electron antineutrinos for energies $\mathcal{O}(10)$ MeV in the gadolinium-loaded Super-Kamiokande (SK) detector. In 2020 June, gadolinium was introduced to the ultrapure water of the SK detector in order to detect neutrons more efficiently. In this new experimental phase, SK-Gd, we can search for electron antineutrinos via inverse beta decay with efficient background rejection thanks to the high efficiency of the neutron tagging technique. In this paper, we report the result for the initial stage of SK-Gd, during 2020 August 26, and 2022 June 1 with a 22.5×552 kton · day exposure at 0.01% Gd mass concentration. No significant excess over the expected background in the observed events is found for the neutrino energies below 31.3 MeV. Thus, the flux upper limits are placed at the 90% confidence level. The limits and sensitivities are already comparable with the previous SK result with pure water (22.5×2970 kton · day) owing to the enhanced neutron tagging. Operation with Gd increased to 0.03% started in 2022 June.

Unified Astronomy Thesaurus concepts: Supernova neutrinos (1666); Neutrino astronomy (1100)

1. Introduction

Astrophysical electron antineutrinos ($\bar{\nu}_e$) are a unique probe to assess various physical phenomena in the universe, such as past supernovae (Beacom 2010), resonant spin flavor precession (RSFP) of solar neutrinos (Akhmedov & Pulido 2003; Díaz et al. 2009), and the annihilation of MeV-scale light dark matter (Palomares-Ruiz & Pascoli 2008), which are expected to appear at energies $\mathcal{O}(10)$ MeV.

The core-collapse supernova (CCSN) is one of the transient processes with the highest neutrino production in our universe. A neutrino observation from CCSN has occurred only once so far, from the supernova SN1987A, by the Kamiokande (Hirata et al. 1987), IMB (Bionta et al. 1987), and Baksan (Alekseev

et al. 1987) neutrino detectors. Although nearby CCSNe are rare, neutrinos from all past supernovae (diffuse supernova neutrino background, DSNB) should exist around us. The theoretical expectations for the DSNB flux depend on various parameters: the supernova rate introduced from the cosmic star formation rate depending on the redshift, the neutrino mass ordering, the equations of states for remnant neutron stars, the metallicity of the galaxy, the failed supernova rate, and the binary interaction effect of stars (Hartmann & Woosley 1997; Malaney 1997; Kaplinghat et al. 2000; Ando et al. 2003; Ando 2005; Horiuchi et al. 2009; Lunardini 2009; Galais et al. 2010; Nakazato et al. 2015; Horiuchi et al. 2018, 2021; Kresse et al. 2021; Tabrizi & Horiuchi 2021; Ekanger et al. 2022). Ashida & Nakazato (2022) have investigated the fraction for the failed CCSNe forming black holes from the DSNB flux upper limit.

The Sun is one of the most intense astrophysical electron neutrino sources at Earth. The solar $\bar{\nu}_e$ can be produced by the combination of the Mikheyev–Smirnov–Wolfenstein (MSW) effect (Smirnov 2005) and the RSFP effect via the neutrino magnetic moment. The limit for the neutrino–antineutrino conversion probability $P_{\nu_e \to \bar{\nu}_e}$ of solar neutrinos due to RSFP was placed from the $\bar{\nu}_e$ flux upper limit by Agostini et al. (2021)

and Abe et al. ([2022a](#), [2022c](#)). In addition, a small flux of the $\bar{\nu}_e$ from the Sun, via the beta decay of ^{40}K, ^{238}U, and ^{232}Th, is predicted by Malaney et al. ([1990](#)), but also has not been observed yet.

Neutrino production from self-annihilation of MeV-scale light-dark-matter particles ($\chi\chi \to \nu\nu$) is also predicted (Argüelles et al. [2021](#)). An upper limit on the averaged cross section for the self-annihilation of the light dark matter is placed from the $\bar{\nu}_e$ flux upper limit by Abe et al. ([2022c](#)).

Although neutrino detectors worldwide have been searching for these events, no significant signal has been found so far. The most stringent upper limits for the astrophysical $\bar{\nu}_e$ flux are set by Super-Kamiokande above 13.3 MeV (Abe et al. [2021](#)) and by KamLAND experiment below 13.3 MeV (Abe et al. [2022c](#)). For further lower-energy regions, the Borexino experiment (Agostini et al. [2021](#)) gave the lowest upper limit below 8.3 MeV. In this paper, we present a new search for astrophysical $\bar{\nu}_e$ in the neutrino energy range of 9.3 to 31.3 MeV based on the observation made with the new Super-Kamiokande detector configuration.

2. The Super-Kamiokande Experiment

Super-Kamiokande (SK; Fukuda et al. [2003](#)) is a water-Cherenkov detector experiment located 1000 m underground in Kamioka, Japan. The detector is of cylindrical shape inside a tank with a diameter of 39.3 m and a height of 41.4 m. It is currently filled with 50 kton of gadolinium-doped ultrapure water (Abe et al. [2022b](#)) as a target. It is optically separated into a main cylindrical volume (inner detector, ID), surrounded by the outer detector (OD) that extends up to the inner surface of the SK tank. SK observes signals of neutrino interactions via the detection of Cherenkov light produced by charged particles within the ID using the ID PMTs. The ID is 33.8 m in diameter and 36.2 m in height, with 11,129 20 inch photomultiplier tubes (PMTs) mounted pointing inwards to the inside of the ID tank. SK is sensitive to neutrinos with an energy range from several MeV to above 1 TeV.

The OD is concentrically placed outside the ID; it is about 2 m wide. It is instrumented with 1885 8 inch PMTs that are mounted on the outer side of the ID structure pointing outwards. The OD surface is covered by white Tyvek sheet to enhance the light reflection in the OD. The OD is primarily utilized to veto cosmic-ray muons.

Since the start of SK operation in 1996, several upgrades to the detector have been carried out. Notably, the electronics were upgraded in 2008 (Yamada et al. [2010](#)) allowing the implementation of a new event trigger, super high energy (SHE), to identify events above ~6 MeV. In addition, the upgrade enables us to record all PMT hits within 535 μs after the SHE-triggered event. The period for which the SHE trigger was implemented is called "SK-IV," and it operated until 2018.

In general, the triggers are issued using the number of ID or OD PMT hits within a 200 ns window. For the SHE trigger, the threshold is typically 60 ID PMT hits. The threshold for the OD trigger is typically 22 OD PMT hits.

Another important upgrade was the loading of Gd into the ultrapure water of SK in order to improve neutron-tagging efficiency due to Gd's high neutron-capture cross section and enhanced neutron-capture signal. The original idea was proposed by Beacom & Vagins ([2004](#)), and the loading was carried out starting in 2020 July. After dissolving gadolinium-sulfate-octahydrate $Gd_2(SO_4)_3 \cdot 8H_2O$ in the ultrapure water

(Abe et al. [2022b](#)), the SK experiment started a new phase called SK-Gd. The initial running period of SK-Gd is called "SK-VI"; it operated with 0.011% Gd mass concentration until 2022 June. Under this condition, about 50% of neutrons are captured by the Gd with a typical time constant of 115 μs. Thermal neutron capture on Gd results in multiple gamma-ray emissions with a total energy of about 8 MeV, which can be easily distinguished from the random backgrounds from natural radioactivity and PMT dark noise. In this paper, 552.2 days of live time taken during SK-VI from 2020 August to 2022 June is used for the $\bar{\nu}_e$ signal search.

3. Event Selection

In this analysis, inverse beta decay (IBD; $\bar{\nu}_e + p \to e^+ + n$) signals from the astrophysical neutrinos are investigated. The signals consist of a positron-like event (prompt event) and a subsequent delayed neutron (delayed signal). We search for IBD signals in the data with the SHE-triggered and successfully recorded 535 μs event from the signal energy region of 7.5–29.5 MeV for the reconstructed kinetic energy of prompt events (E_{rec}). In addition, the condition that the OD trigger is not issued is also required in order to remove incoming cosmic-ray muon events.

The event selection and reconstruction follow the previous SK-IV search (Abe et al. [2021](#)), except for the delayed neutron identification. Prompt events with exactly one delayed-tagged neutron signal are selected as IBD signal candidates. Those neutron signals are searched for within a 535 μs window after the prompt event. In SK-Gd, the neutron signal from thermal neutron capture on the Gd nucleus is efficiently tagged by a simple signal selection without using the machine-learning-based cut used in previous analysis (Abe et al. [2021](#)).

As a primary selection, an algorithm searching for PMT hit clusters within 200 ns windows is applied. In this stage, the clusters with 25 hits or more are selected as candidates for neutron signals. Then, basic event reduction cuts, used in common with the analysis for the $\mathcal{O}(10)$ MeV scale in SK, are applied. The cuts include the goodness of reconstruction, the electron likeness of the Cherenkov ring hit pattern, and the fiducial volume cut that requires the event to be further than 2 m from the wall.

For further reduction, we apply a "distance" cut and an "energy" cut. The reconstructed vertex of the delayed signal tends to be close to the prompt event for the IBD interactions of $\mathcal{O}(10)$ MeV neutrinos. Thus the distance between the prompt and delayed signal candidate is an efficient discriminator to select neutron events. In this analysis, the candidates that have a distance of over 3 m from the prompt event vertex are eliminated. Also, the reconstructed energy of multiple gamma-ray events from Gd capture is typically around 4–5 MeV, as shown in Harada ([2022](#)). After the 3 m distance cut, the remaining background events are low-energy accidental backgrounds due to noise hits. Hence a 3.5 MeV energy threshold is assigned in order to reduce the accidental coincidence rate to $\mathcal{O}(10^{-4})$ per event.

Neutron tagging efficiency and the misidentification probability are estimated by applying the above selection procedure to neutron signals simulated by a Monte Carlo (MC) simulation based on Geant4.10.5p1 (Allison et al. [2006](#)), and SK random trigger data, respectively. The Gd concentration in the MC simulation is tuned to reproduce the time constant of the measured data. For the gamma-ray emission from thermal
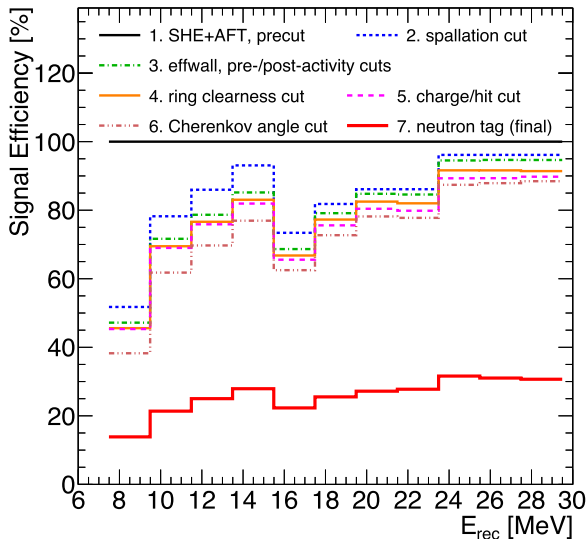
Figure 1. IBD signal efficiency for the signal energy region. The 100% efficiency line corresponds to data after trigger requirements and noise reduction cuts. These lines show the cumulative efficiency at each cut stage, performed in the order shown in the legend. More detailed explanations for each reduction step, except for the neutron tagging, are described in Abe et al. (2021).

neutron capture on Gd in MC simulation, the ANNRI-Gd model (Hagiwara et al. 2019; Tanaka et al. 2020) is utilized. The selection efficiency of the Gd capture signal is evaluated to be $73.2\% \pm 0.2\%$. Given that the capture fraction on Gd is $47.8\% \pm 0.2\%$ and systematic uncertainty estimated based on Harada (2022), the total neutron tagging efficiency is estimated to be $35.\%6 \pm 2.5\%$. The misidentification probability of noise candidates $\varepsilon_{\rm mis}$ is found to be $(2.8 \pm 0.1) \times 10^{-4}$ per event. It is sufficiently low to remove most accidental coincidences. In the previous analysis (Abe et al. 2021), typical neutron tagging efficiency and the misidentification probability using a boosted decision tree (Chen & Guestrin 2016) were about 20% and also $\mathcal{O}(10^{-4})$, respectively.

Figure 1 shows the total IBD signal efficiency for each 2 MeV $E_{\rm rec}$ bin. The efficiencies after each of the main selection criteria applied are shown together.

The signal efficiency after neutron tagging (the red line in Figure 1) is about twice that of the previous SK search (shown in the upper panel of Figure 18 in Abe et al. 2021), especially below 15.49 MeV, thanks to the higher neutron detection efficiency.

A large part of the accidental coincidence background originates from pairs of events from the decay of isotopes produced by muon spallation induced by the cosmic-ray muon and the low-energy noise events. Therefore, efficient spallation event reduction and low $\varepsilon_{\rm mis}$ in neutron tagging are important to reduce the accidental coincidence background. Thus, the spallation cut criteria are optimized in each energy range to remove various isotope decays at the corresponding energy. Because of the lower $\varepsilon_{\rm mis}$ than for SK-IV, we reoptimized the spallation cut criteria below 15.49 MeV, where we have large enough statistics of the spallation sample. As a result, the spallation cut condition was loosened to achieve higher signal efficiency. On the other hand, the spallation cut criteria cannot be optimized above 15.49 MeV because there are fewer spallation samples. In order to avoid possible systematics due to misestimating the spallation backgrounds in this region, harder spallation cut with lower signal efficiency was

applied to almost completely eliminate spallation events above 15.49 MeV.

The side-band region above 29.49 MeV is used as the reference for the atmospheric neutrino events. The efficiency in this region is stable and almost the same as for the 27.49–29.49 MeV bin.

4. Background Estimation

Major background sources in the signal energy region are atmospheric neutrino interaction events, reactor neutrino events, and decays of spallation isotopes produced by cosmic-ray muon events. The solar neutrinos, which predominantly interact via electron scattering in SK, have no subsequent neutron signal. Thus, requiring one neutron makes the solar neutrino background negligible. Another background source is accidental background events, which are a pair of prompt SHE events and a misidentified delayed signal due to PMT noise hits or radioactivity.

Spallation isotope decays other than the $\beta + n$ decay are efficiently removed by the spallation event cut and neutron tagging. ^{8}He, ^{11}Li, ^{16}C, and ^{9}Li are the representative decay isotopes that undergo $\beta + n$ decay. However, ^{11}Li is negligible since it can be removed by the spallation cut efficiently due to its short life ($T_{1/2} < 0.01$ s), and its production yield is low ($10^{-9}\,\mu^{-1}\,{\rm g}^{-1}\,{\rm cm}^2$; Li & Beacom 2014). Also, ^{8}He and ^{16}C have a low production yield of about 0.23×0.16 and $0.02 \times 10^{-7}\,\mu^{-1}\,{\rm g}^{-1}\,{\rm cm}^2$ (Li & Beacom 2014). In contrast, ^{9}Li has a relatively long life ($T_{1/2} \sim 0.18$ s), so it is difficult to identify its parent muon. In addition, the production yield is sufficiently higher, about $1.9 \times 0.51 \times 10^{-7}\,\mu^{-1}\,{\rm g}^{-1}\,{\rm cm}^2$ (Li & Beacom 2014), where 0.51 comes from the branching ratio for this decay mode. Thus, we consider only ^{9}Li as the remaining background from the spallation isotope decays. The production yield of ^{9}Li event is measured to be 0.86 ± 0.12 (stat.) $\pm$ 0.15 (sys.) $\rm kton^{-1} \cdot day^{-1}$ by Zhang et al. (2016), and a prediction of the spectrum is given in Abe et al. (2021).

Reactor $\bar{\nu}_e$ inevitably remains in the final signal candidates since the observed event is IBD, which is the same as our target signal. The spectrum and yield are evaluated by the SKReact code (Goldsack 2022) based on the reactor neutrino model from Baldoncini et al. (2015) in the first 7.5–9.5 MeV $E_{\rm rec}$ bin. Their contribution above the 9.5 MeV $E_{\rm rec}$ bin is negligible.

The number of atmospheric neutrino background events is estimated by the simulation based on the HKKM flux (Honda et al. 2007, 2011) as the neutrino flux and NEUT 5.4.0.1 (Hayato 2009; Hayato & Pickering 2021) as the neutrino interaction simulator. Below 16 MeV of $E_{\rm rec}$, nuclear deexcitation gamma-rays from neutral-current quasi-elastic (NCQE) interactions dominate (Ankowski et al. 2012). NCQE interactions induce prompt gamma-rays and nuclei production. Above 16 MeV, it is dominated by charged-current quasi-elastic (CCQE) interactions with neutron production. Most of the events with $E_{\rm rec}$ from 29.5 to 79.5 MeV consist of the decay electron from an unobserved muon originating from CCQE interacting atmospheric neutrinos. Since its energy distribution is the well-known Michel spectrum, the flux of atmospheric neutrino CCQE events in our MC is scaled by fitting the spectrum of the $29.5 < E_{\rm rec} < 79.5$ MeV side-band region to the data.

The number of accidental coincidence background events B_{acc} is estimated as

$$B_{\mathrm{acc}} = \varepsilon_{\mathrm{mis}} \times N_{\mathrm{pre-ntag}}^{\mathrm{data}}, \qquad (1)$$

where $\varepsilon_{\mathrm{mis}}$ is the neutron misidentification probability described in Section 3, and $N_{\mathrm{pre-ntag}}^{\mathrm{data}}$ represents the number of remaining observed events after all selection criteria except neutron tagging.

Systematic uncertainties are estimated for only signal energy regions. The uncertainties on the NCQE events, spallation ^{9}Li, and reactor neutrinos are taken as estimated by Abe et al. (2021), as 68% below 15.49 MeV and 82% above 15.49 MeV, 60%, and 100% for the NCQE, ^{9}Li, and reactor neutrino backgrounds, respectively. Other components, such as non-NCQE events and accidental coincidence events, are newly estimated from the observed data in SK-VI based on the same method as Abe et al. (2021), 44% and 4%, respectively.

5. Results

After all event selection criteria are applied, 16 events remain within the signal energy region in 552.2 day data. In this analysis, we adopt five separate bins of E_{rec}, of widths 7.5–9.5, 9.5–11.5, 11.5–15.5, 15.5–23.5, and 23.5–29.5 MeV for the signal window. Also, the side-band region is separated into bins for each 10 MeV. Figure 2 shows the E_{rec} spectrum of those events. This is also listed in Table 1.

The probabilities of finding the observed number of events due to the fluctuation of the background events (p-value) are evaluated for each bin. It is done by performing 10^6 pseudo experiments based on the number of observed events and expected background events and the systematic uncertainties of the latter. The obtained p-values are listed in Table 1. We conclude that no significant excess is observed in the data over the expected background since even the most significant bin has a p-value is 25.8%.

We set the upper limit for the number of signal excess over the expected background with a 90% confidence level (C.L.; N_{90}). It is evaluated by the pseudo experiments using the number of observed events with these 1σ statistical uncertainties and the number of expected background events with their systematic uncertainties. Then we estimate the flux upper limit based on N_{90} of the observed event. Assuming there is no signal event, the upper limit on the flux for each bin is calculated as

$$\phi_{90}^{\mathrm{limit}} = \frac{N_{90}}{\bar{\sigma}_{\mathrm{IBD}} \cdot N_p \cdot T \cdot \bar{\varepsilon}_{\mathrm{sig}} \cdot dE}. \qquad (2)$$

Here, $\bar{\sigma}_{\mathrm{IBD}}$ is the averaged total cross section of IBD for each energy bin, N_p is the number of protons as a target in the 22.5 kton of the fiducial volume of SK, T is the live time of observation (552.2 days), $\bar{\varepsilon}_{\mathrm{sig}}$ is the averaged signal efficiency for each energy bin after all event selection criteria are applied as shown in Figure 1, and dE is the bin width at each bin. The neutrino energy E_ν is calculated by $E_\nu = E_{\mathrm{rec}} + 1.8$ MeV. The total cross section is given by the calculation in Strumia & Vissani (2003).

The expected upper limit from the background-only hypothesis at 90% C.L., $N_{90,\,\mathrm{exp}}$, is evaluated using the number of expected background events and their statistical uncertainty. Then we extract the expected flux sensitivity by replacing N_{90} with $N_{90,\,\mathrm{exp}}$ in Equation (2).
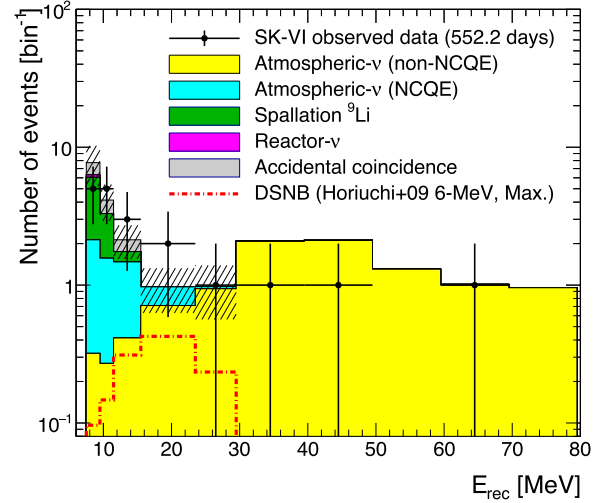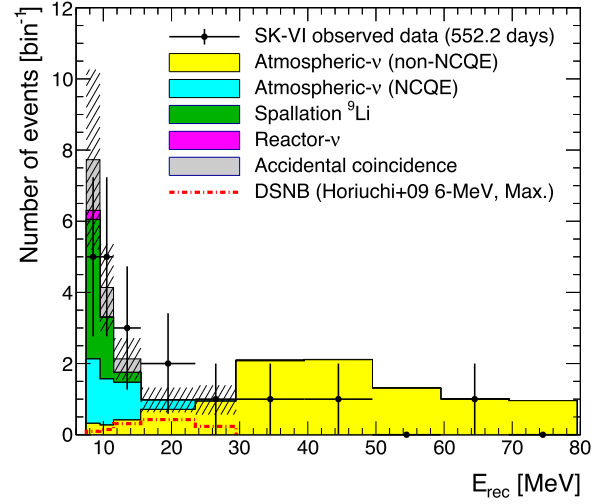

Figure 2. Reconstructed energy spectra of the observed data and the expected background after data reductions with a linear (top) and a logarithmic (bottom) scale for the vertical axis. These include the signal energy region and the side-band region above 29.5 MeV. Each color-filled histogram shows the expected backgrounds. The error bars in the data points represent the statistical uncertainty estimated by taking the square root of the number of observed events. These background histograms are stacked on the other histograms. The hatched areas represent the total systematic uncertainty for each bin. The size of uncertainty for each background is mentioned in the main text. The red dotted–dashed line shows the DSNB expectation from the Horiuchi+09 model (Horiuchi et al. 2009), which is drawn separately from the stacked histogram of the estimated backgrounds.

Table 1
Summary of Observed Events, Expected Background Events, and p-value for Each E_{rec} Bin

E_{rec} (MeV)	Observed	Expected	p-value
7.5–9.5	5	7.73 ± 2.54	0.798
9.5–11.5	5	4.14 ± 1.23	0.398
11.5–15.5	3	2.13 ± 0.59	0.359
15.5–23.5	2	0.98 ± 0.35	0.258
23.5–29.5	1	0.98 ± 0.41	0.597

Note. Errors for the expected background represent only the systematic uncertainty.

Figure 3 shows the upper limit of the $\bar{\nu}_e$ flux extracted in this search with the range of expectations of modern DSNB models. The most optimistic expectation is Kaplinghat+00 (Kaplinghat
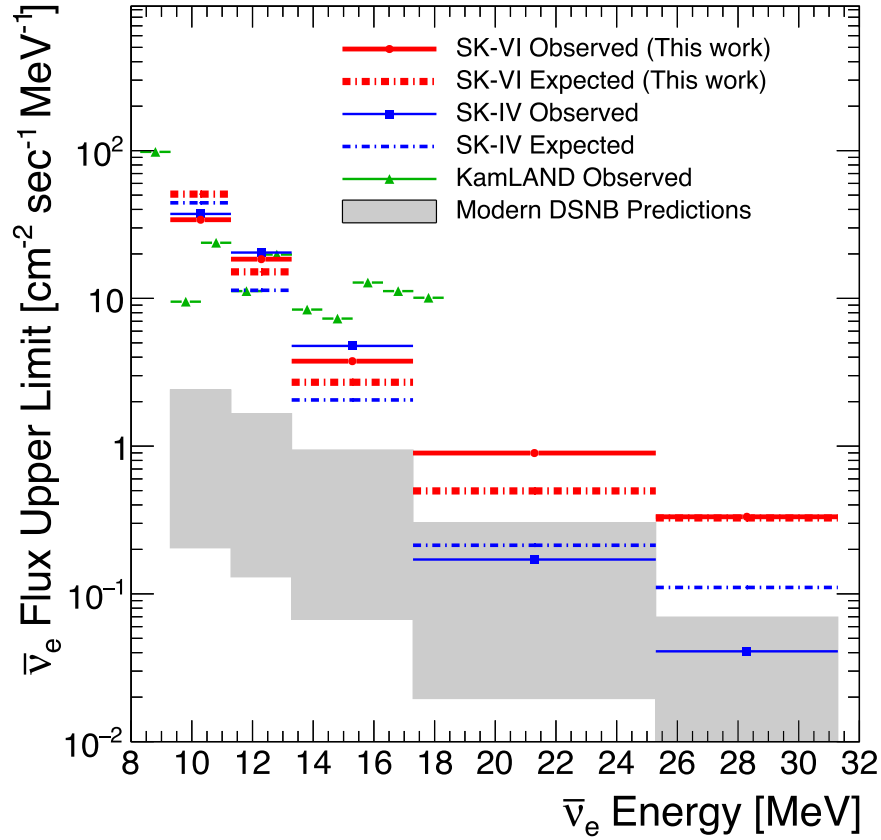
Figure 3. Upper limits on the $\bar{\nu}_e$ flux, calculated by Equation (2). The red lines show the observed (solid) and expected (dotted–dashed) 90% C.L. upper limit for SK-VI. The blue lines show the observed (solid) and expected (dotted–dashed) 90% C.L. upper limit for SK-IV Abe et al. (2021). The green line represents the 90% C.L. observed upper limit placed by KamLAND Abe et al. (2022c). The gray-shaded region represents the range of the modern theoretical expectation. The expectation drawn in the figure includes DSNB flux models (Hartmann & Woosley 1997; Malaney 1997; Kaplinghat et al. 2000; Ando et al. 2003; Horiuchi et al. 2009; Lunardini 2009; Galais et al. 2010; Nakazato et al. 2015; Horiuchi et al. 2018, 2021; Kresse et al. 2021; Tabrizi & Horiuchi 2021; Ekanger et al. 2022). Ando+03 model was updated in Ando (2005).

Table 2
Summary Table of Upper Limits, Sensitivity, and Optimistic and Pessimistic DSNB Expectation from Kaplinghat et al. (2000) and Nakazato et al. (2015), Respectively

Neutrino Energy (MeV)	Observed upper limit (cm^{-2} s^{-1} MeV^{-1})		Expected sensitivity (cm^{-2} s^{-1} MeV^{-1})		Averaged theoretical expectation of DSNB (cm^{-2} s^{-1} MeV^{-1})
	SK-IV	SK-VI	SK-IV	SK-VI	
9.29–11.29	37.30	34.07	44.35	50.78	0.20–2.40
11.29–13.29	20.43	18.43	11.35	15.12	0.13–1.66
13.29–17.29	4.77	3.76	2.05	2.71	0.67–0.94
17.29–25.29	0.17	0.90	0.21	0.50	0.02–0.30
25.29–31.29	0.04	0.33	0.11	0.33	<0.01–0.07

et al. 2000), and the most pessimistic one is Nakazato+15 (Nakazato et al. 2015) with the assumption of normal mass ordering in whole energy ranges, respectively. The upper limit of the flux for each bin is summarized in Table 2.

6. Future Prospects

In 2022 June, the SK-Gd experiment was upgraded to the SK-VII phase, in which additional Gd was introduced into the detector, providing a mass concentration of approximately 0.03%. In this phase, neutron tagging efficiency is expected to be over 55% while having comparable ε_{mis} with SK-VI, leading to 1.5 times higher sensitivity for the $\bar{\nu}_e$ in the case of the same live time as for SK-VI. Furthermore, more efficient noise reduction by neutron tagging will enable a lower energy

threshold. Hence we can search in a lower-energy region, which will increase signal acceptance for DSNB, solar antineutrinos, and light-dark-matter searches.

7. Conclusions

We searched for astrophysical $\bar{\nu}_e$, using the SK-VI data below 29.5 MeV for E_{rec} between 2020 August and 2022 May, with 0.01% Gd mass concentration. This is an independent data set from the previous SK-IV search (Abe et al. 2021), using the data taken with pure water. In this analysis, a brand-new method for tagging neutrons using the signal of neutron capture on Gd is utilized so that the efficiency of neutron tagging is twice as high while keeping a low-misidentification probability. No significant excess above the expected backgrounds at

greater than 90% C.L. level for five separate energy bins between 9.3 and 31.3 MeV is found. Thus, we placed the upper limits on the $\bar{\nu}_e$ flux for the observed upper limit and the expected sensitivity. The sensitivity of this work is comparable to the previous SK-IV search (Abe et al. 2021) with a live time of 2970 days, which is the world's most sensitive search above 13.3 MeV, even though the live time of 552.2 days is about 5 times smaller. The result was achieved by neutron tagging with Gd signal and lowered probability of accidental coincidences thanks to the benefit of introducing Gd.

ORCID iDs

M. Harada https://orcid.org/0000-0003-3273-946X
C. Bronner https://orcid.org/0000-0001-9555-6033
Y. Hayato https://orcid.org/0000-0002-8683-5038
K. Hiraide https://orcid.org/0000-0003-1229-9452
K. Hosokawa https://orcid.org/0000-0002-8766-3629
K. Ieki https://orcid.org/0000-0002-7791-5044
M. Ikeda https://orcid.org/0000-0002-4177-5828
Y. Kataoka https://orcid.org/0000-0001-9090-4801
S. Moriyama https://orcid.org/0000-0001-7630-2839
Y. Nakano https://orcid.org/0000-0003-1572-3888
M. Nakahata https://orcid.org/0000-0001-7783-9080
S. Nakayama https://orcid.org/0000-0002-9145-714X
Y. Noguchi https://orcid.org/0000-0002-3113-3127
H. Sekiya https://orcid.org/0000-0001-9034-0436
M. Shiozawa https://orcid.org/0000-0003-0520-3520
Y. Takemoto https://orcid.org/0000-0003-2232-7277
T. Yano https://orcid.org/0000-0002-5320-1709
K. Okumura https://orcid.org/0000-0002-5523-2808
T. Tashiro https://orcid.org/0000-0003-1440-3049
P. Fernandez https://orcid.org/0000-0001-9034-1930
L. Labarga https://orcid.org/0000-0002-6395-9142
N. Ospina https://orcid.org/0000-0002-8404-1808
L. Wan https://orcid.org/0000-0001-5524-6137
T. Wester https://orcid.org/0000-0001-6668-7595

N. J. Griskevich https://orcid.org/0000-0003-4409-3184
H. W. Sobel https://orcid.org/0000-0001-5073-4043
A. Yankelevich https://orcid.org/0000-0002-5963-3123
B. Bodur https://orcid.org/0000-0001-8454-271X
K. Scholberg https://orcid.org/0000-0002-7007-2021
C. W. Walter https://orcid.org/0000-0003-2035-2380
Th. A. Mueller https://orcid.org/0000-0003-2743-4741
P. Paganini https://orcid.org/0000-0001-9580-683X
N. Iovine https://orcid.org/0000-0001-7965-2252
M. Scott https://orcid.org/0000-0002-1759-4453
V. Berardi https://orcid.org/0000-0002-8387-4568
N. F. Calabria https://orcid.org/0000-0003-3590-2808
A. Langella https://orcid.org/0000-0001-6273-3558
L. N. Machado https://orcid.org/0000-0002-7578-4183
G. Collazuol https://orcid.org/0000-0002-7876-6124
F. Iacob https://orcid.org/0000-0003-3582-3819
M. Mattiazzi https://orcid.org/0000-0003-3900-6816
G. Pronost https://orcid.org/0000-0001-6429-5387
Y. Nishimura https://orcid.org/0000-0002-7666-3789
T. Hasegawa https://orcid.org/0000-0002-2967-1954
T. Matsubara https://orcid.org/0000-0003-3187-6710
Y. Oyama https://orcid.org/0000-0002-1689-0285
F. Di Lodovico https://orcid.org/0000-0003-3952-2175
T. Katori https://orcid.org/0000-0002-9429-9482
J. Migenda https://orcid.org/0000-0002-5350-8049
S. Zsoldos https://orcid.org/0000-0003-0142-4844
Y. Takeuchi https://orcid.org/0000-0002-4665-2210
J. R. Hu https://orcid.org/0000-0003-2149-9691
Z. Hu https://orcid.org/0000-0002-0353-8792
T. Nakaya https://orcid.org/0000-0003-3040-4674
R. A. Wendell https://orcid.org/0000-0002-0969-4681
S. J. Jenkins https://orcid.org/0000-0002-0982-8141
N. McCauley https://orcid.org/0000-0002-5982-5125
A. Tarrant https://orcid.org/0000-0002-8750-4759
Y. Fukuda https://orcid.org/0000-0003-2660-1958
Y. Itow https://orcid.org/0000-0002-8198-1968
H. Menjo https://orcid.org/0000-0001-8466-1938
C. Yanagisawa https://orcid.org/0000-0002-6490-1743
Y. Hino https://orcid.org/0000-0002-7480-463X
Y. Koshio https://orcid.org/0000-0003-0437-8505
F. Nakanishi https://orcid.org/0000-0003-4408-6929
S. Sakai https://orcid.org/0000-0002-2190-0062
D. Barrow https://orcid.org/0000-0001-5844-709X
F. Nova https://orcid.org/0000-0002-0769-9921
B. S. Yang https://orcid.org/0000-0001-5877-6096
J. Y. Yang https://orcid.org/0000-0002-3624-3659
J. Yoo https://orcid.org/0000-0002-3313-8239
L. Kneale https://orcid.org/0000-0002-4087-1244
M. D. Thiesse https://orcid.org/0000-0002-0775-250X
E. Kwon https://orcid.org/0000-0001-5653-2880
J. W. Seo https://orcid.org/0000-0002-2719-2079
I. Yu https://orcid.org/0000-0003-1567-5548
K. D. Nakamura https://orcid.org/0000-0003-3302-7325
S. Tairafune https://orcid.org/0000-0002-2140-7171
K. Nishijima https://orcid.org/0000-0002-1830-4251
Y. Nakajima https://orcid.org/0000-0002-2744-5216
M. Yokoyama https://orcid.org/0000-0003-2742-0251
P. de Perio https://orcid.org/0000-0002-0741-4471
M. R. Vagins https://orcid.org/0000-0002-0569-0480
M. Kuze https://orcid.org/0000-0001-8558-8440
S. Izumiyama https://orcid.org/0000-0002-0808-8022
R. Matsumoto https://orcid.org/0000-0002-4995-9242

H. Ito https://orcid.org/0000-0003-1029-5730
M. Shinoki https://orcid.org/0000-0002-9486-6256
N. W. Prouse https://orcid.org/0000-0003-1037-3081
B. D. Xu https://orcid.org/0000-0001-5135-1319
M. Posiadala-Zezula https://orcid.org/0000-0002-5154-5348
Ll. Marti https://orcid.org/0000-0002-5172-9796
A. Minamino https://orcid.org/0000-0001-6510-7106

References

Abe, K., Bronner, C., Hayato, Y., et al. 2021, PhRvD, 104, 122002
Abe, K., Bronner, C., Hayato, Y., et al. 2022a, APh, 139, 102702
Abe, K., Bronner, C., Hayato, Y., et al. 2022b, NIMPA, 1027, 166248
Abe, S., Asami, S., Gando, A., et al. 2022c, ApJ, 925, 14
Agostini, M., Altenmüller, K., Appel, S., et al. 2021, APh, 125, 102509
Akhmedov, E. K., & Pulido, J. 2003, PhLB, 553, 7
Alekseev, E. N., Alekseeva, L. N., Volchenko, V. I., & Krivosheina, I. V. 1987, JETPL, 45, 589
Allison, J., Amako, K., Apostolakis, J., et al. 2006, ITNS, 53, 270
Ando, S., Sato, K., & Totani, T. 2003, NuPhA, 721, C541
Ando, S. I. 2005, Proc. of the Next Generation of Nucleon Decay and Neutrino Detectors, SLAC eConf No. C0504071, ed. J. Dumarchez, (Stanford, CA: Stanford Univ.)
Ankowski, A. M., Benhar, O., Mori, T., Yamaguchi, R., & Sakuda, M. 2012, PhRvL, 108, 052505
Argüelles, C. A., Diaz, A., Kheirandish, A., et al. 2021, RvMP, 93, 035007
Ashida, Y., & Nakazato, K. 2022, ApJ, 937, 30
Baldoncini, M., Callegari, I., Fiorentini, G., et al. 2015, PhRvD, 91, 065002
Beacom, J. F. 2010, ARNPS, 60, 439
Beacom, J. F., & Vagins, M. R. 2004, PhRvL, 93, 171101
Bionta, R. M., Blewitt, G., Bratton, C. B., et al. 1987, PhRvL, 58, 1494
Chen, T., & Guestrin, C. 2016, in 22nd ACM SIGKDD Int. Conf. on Knowledge Discovery and Data Mining (San Francisco, CA: Association for Computing Machinery), 785

Díaz, J. S., Kostelecký, V. A., & Mewes, M. 2009, PhRvD, 80, 076007
Ekanger, N., Horiuchi, S., Kotake, K., & Sumiyoshi, K. 2022, PhRvD, 106, 043026
Fukuda, S., Fukuda, Y., Hayakawa, T., et al. 2003, NIMPA, 501, 418
Galais, S., Kneller, J., Volpe, C., & Gava, J. 2010, PhRvD, 81, 053002
Goldsack, A. 2022, SKReact, Git Hub, https://github.com/Goldie643/SKReact
Hagiwara, K., Yano, T., Tanaka, T., et al. 2019, PTEP, 2019, 023D01
Harada, M. 2022, in 41st Int. Conf. on High Energy Physics (Trieste: SISSA), 1178
Hartmann, D. H., & Woosley, S. E. 1997, APh, 7, 137
Hayato, Y. 2009, AcPPB, 40, 2477
Hayato, Y., & Pickering, L. 2021, EPJST, 230, 4469
Hirata, K., Kajita, T., Koshiba, M., et al. 1987, PhRvL, 58, 1490
Honda, M., Kajita, T., Kasahara, K., & Midorikawa, S. 2011, PhRvD, 83, 123001
Honda, M., Kajita, T., Kasahara, K., Midorikawa, S., & Sanuki, T. 2007, PhRvD, 75, 043006
Horiuchi, S., Beacom, J. F., & Dwek, E. 2009, PhRvD, 79, 083013
Horiuchi, S., Kinugawa, T., Takiwaki, T., Takahashi, K., & Kotake, K. 2021, PhRvD, 103, 043003
Horiuchi, S., Sumiyoshi, K., Nakamura, K., et al. 2018, MNRAS, 475, 1363
Kaplinghat, M., Steigman, G., & Walker, T. P. 2000, PhRvD, 62, 043001
Kresse, D., Ertl, T., & Janka, H.-T. 2021, ApJ, 909, 169
Li, S. W., & Beacom, J. F. 2014, PhRvC, 89, 045801
Lunardini, C. 2009, PhRvL, 102, 231101
Malaney, R. A. 1997, APh, 7, 125
Malaney, R. A., Meyer, B. S., & Butler, M. N. 1990, ApJ, 352, 767
Nakazato, K., Mochida, E., Niino, Y., & Suzuki, H. 2015, ApJ, 804, 75
Palomares-Ruiz, S., & Pascoli, S. 2008, PhRvD, 77, 025025
Smirnov, A. Y. 2005, PhST, 121, 57
Strumia, A., & Vissani, F. 2003, PhLB, 564, 42
Tabrizi, Z., & Horiuchi, S. 2021, JCAP, 2021, 011
Tanaka, T., Hagiwara, K., Gazzola, E., et al. 2020, PTEP, 2020, 043D02
Yamada, S., Awai, K., Hayato, Y., et al. 2010, ITNS, 57, 428
Zhang, Y., Abe, K., Haga, Y., et al. 2016, PhRvD, 93, 012004